Available online at www.sciencedirect.com
ScienceDirect
Applied Catalysis B: Environmental 79 (2008) 307–312
APPLIED CATALYSIS B: ENVIRONMENTAL
www.elsevier.com/locate/apcatb

# Biomorphic SiC pellets as catalyst support for partial oxidation of methane to syngas

Qing Wang [a,b], Wei-Zhong Sun [a,b], Guo-Qiang Jin [a], Ying-Yong Wang [a], Xiang-Yun Guo [a,*]

[a] State Key Laboratory of Coal Conversion, Institute of Coal Chemistry, Taiyuan 030001, PR China
[b] Graduate School of the Chinese Academy of Sciences, Beijing 100039, PR China

Received 5 June 2007; received in revised form 16 October 2007; accepted 29 October 2007
Available online 4 November 2007

**Abstract**

Biomorphic silicon carbide (bioSiC) pellets prepared from carbonized millet were employed as nickel catalyst support for the partial oxidation of methane to syngas in a fixed-bed quartz reactor at 800 °C. To reduce the loss of nickel active component during the reaction, alumina was used to modify the bioSiC surface. The temperature programmed reduction reveals that the alumina modification can evidently increase the reduction temperature of nickel oxide and therefore enhance the interaction between nickel and support. Due to the enhanced interaction, the nickel component becomes stable and difficult to migrate on the support surface. As a result, the modified bioSiC catalyst shows higher catalytic activity and stability than the unmodified. Compared with the catalyst supported on powdered SiC, the pelletized catalyst shows higher activity, especially at high gas hourly space velocity.


*Keywords:* Partial oxidation of methane; Ni/bioSiC catalyst; Ni/bioSiC–$Al_2O_3$ catalyst

## 1. Introduction

Converting methane to syngas has received significant attention in recent years [1–5]. Nowadays, different routes have been proposed for the methane conversion, such as steam reforming, $CO_2$ reforming and partial oxidation [6]. Among these routes, the catalytic partial oxidation of methane (POM) is recognized as a promising route due to the low energy consumption, high efficiency and suitable $H_2$/CO ratio in the product, which is favorable to methanol and Fischer–Tropsch synthesis [7,8].

Catalytic performance of different noble and common metals has been investigated for the POM reaction [7,9–11]. Among them nickel is most frequently studied because of its low cost and high activity [2,5,8]. Through sieving a series of support materials, alumina is generally regarded as the most prospective candidate by the present time [2,4,12]. However the acidity of alumina surface is so strong that Ni/$Al_2O_3$ catalyst is easily deactivated due to the coke deposition [13]. Additionally, nickel component easily reacts with alumina and produces $NiAl_2O_4$, which is lowly active for POM and difficult to reverse back to active nickel component [12,14]. Silicon carbide is a kind of covalent compound and has excellent thermal conductivity, thermal stability and chemical inertness [15], and therefore is regarded as a potential candidate for catalyst support. Several groups have employed SiC as catalyst support for different reactions, such as selective oxidation of $H_2S$, dehydrogenation of *n*-butane and exhaust gas treatment for heavy-duty engines [16–19]. Recently, SiC has also been used for the POM reaction [20,21]. The results indicate that Ni/SiC catalyst has excellent activity and stability. In addition, the catalyst can directly be used in the reaction without pre-reduction and easily be regenerated through burning carbon in air [21]. However, the utilization of SiC as the POM catalyst support is still restricted by several problems. For examples, metal particles over SiC surface easily migrate and grow due to the weak interaction between metal and SiC surface, and this may result in the loss of active component and the decrease of active sites. In addition, powdered SiC is difficult to be shaped due to the chemical inertness of SiC. Obviously, the solution of these problems will greatly accelerate the application of SiC in the POM process.

* Corresponding author. Tel.: +86 351 4065282; fax: +86 351 4050320.
*E-mail address:* xyguo@sxicc.ac.cn (X.-Y. Guo).

0926-3373/$ – see front matter © 2007 Elsevier B.V. All rights reserved.
doi:10.1016/j.apcatb.2007.10.032

Natural biomasses possess complex hierarchical structures characterized by orderly arranged pores with various diameters ranging from nanometer to millimeter scale [22–26]. These structures are developed and optimized in the long evolution process, and thus can offer a highly efficient system for transportation of biologic matters. Similarly, catalyst pellets with hierarchically porous structures are also very interesting for heterogeneously catalytic reactions. The microspores in the pellets can provide plentiful surface and thus accommodate enough active sites while the large pores give a large effective diffusivity [27,28]. Therefore inorganic materials with porous structures similar to those of biomasses will find widespread applications in catalysis, separation and other relative fields.

Recently many of biomasses have been employed to fabricate their inorganic replicas, such as SiC, TiC and $Al_2O_3$ [23,24,29]. We have also converted natural millet into biomorphic silicon carbide (bioSiC) pellets. The bioSiC pellets have a diameter of 1–2 mm, a specific surface area of about 30 $m^2$/g and average crush strength of 10.6 N per grain [24]. In this paper the bioSiC pellets were employed as the catalyst support for POM. Additionally, the SiC surface was modified by alumina to enhance the interaction between nickel active component and support surface.

## 2. Experimental

### 2.1. Catalyst preparation

Pelletized Ni/bioSiC and Ni/bioSiC–$Al_2O_3$ catalysts were prepared by impregnation method. For the Ni/bioSiC catalyst with 10 wt% Ni-loading, the preparation was briefly described as follows. The bioSiC pellets were placed in an infiltration vessel with 10 wt% $Ni(NO_3)_2$ aqueous solution, then the vessel pressure was increased to 1.0 MPa. After 10 h, the mixture was dried at 100 °C and calcined in air at 700 °C for 3 h. The treatment procedure of impregnation, drying and calcining was repeated several times until the mass ratio of NiO to SiC approached to 10%. The preparation of Ni/bioSiC–$Al_2O_3$ catalyst was similar to that of Ni/bioSiC catalyst. The difference was that the infiltration solution in the vessel was a mixed solution of $Ni(NO_3)_2$ (10 wt%) and $Al(NO_3)_3$ (25.6 wt%). By the above procedure, the Ni/bioSiC–$Al_2O_3$ catalyst was prepared with 10 wt% NiO and 15 wt% $Al_2O_3$.

Powdered Ni/SiC–$Al_2O_3$ catalyst with 10 wt% NiO and 15 wt% $Al_2O_3$ was prepared as follows. 0.42 g SiC was added into 50 ml of $Ni(NO_3)_2$ (0.27 wt%) and $Al(NO_3)_3$ (0.7 wt%) mixed solution under stirring. Afterward the mixture was dried at 100 °C and then calcined in air at 700 °C for 3 h.

The preparation of Ni/$Al_2O_3$ catalyst can be found elsewhere [30].

### 2.2. Catalyst test

The catalytic performance of three catalysts was respectively evaluated in a fixed-bed quartz reactor with an interior diameter of 8 mm. A mixture of methane and oxygen (molar ratio ~2.0, no diluent gas) was switched to the reactor with different gas hourly space velocities. The reaction temperature was increased to 800 °C at a rate of 10 °C $min^{-1}$, and the reaction was operated at atmospheric pressure. The composition of effluent gases was analyzed by GC-14B gas chromatograph with TDX-01 column and TCD detector.

### 2.3. Catalyst characterization

The crystalline phases of catalysts were characterized by X-ray diffraction (XRD, Rigaku D-Max/RB, Cu Kα radiation). The catalyst morphologies were observed using scanning electron microscope (SEM, LEO-438VP) equipped with energy dispersive X-ray (EDX). The nickel amount of catalysts was measured by ICP spectrometer (Atomscan 16). The carbon deposition over used catalysts was measured by thermogravimetric analysis (TGA, Perkin-Elmer TGA7). Temperature programmed reduction (TPR) with $H_2$ (10% $H_2$ in $N_2$) was performed with a heating rate of 10 °C $min^{-1}$.

## 3. Results and discussion

### 3.1. XRD characterization of fresh catalysts

Both Ni/bioSiC and Ni/bioSiC–$Al_2O_3$ catalysts were prepared by impregnation method. Due to the $Al_2O_3$ modification, Ni/bioSiC–$Al_2O_3$ catalyst has a higher specific surface area of 41 $m^2$/g than Ni/bioSiC catalyst, which has a specific surface area of 30 $m^2$/g. The two fresh catalysts were firstly analyzed by the XRD technique. From the XRD patterns shown in Fig. 1, the diffraction peaks from $Al_2O_3$ almost cannot be seen, indicating that the $Al_2O_3$ component has been uniformly dispersed on the SiC surface. Additionally, the metal component exists as NiO in the two catalysts. Using Scherrer's formula, the crystalline sizes of NiO ((0 1 2) crystalline face) particles in Ni/bioSiC–$Al_2O_3$ and Ni/bioSiC catalysts are 21.0 nm and 22.8 nm, respectively. The value for Ni/bioSiC–

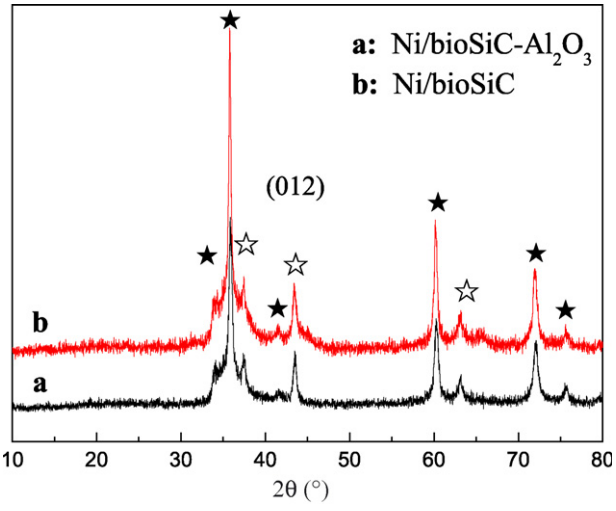


Fig. 1. XRD patterns of fresh catalysts. (★) SiC; (☆) NiO.

$Al_2O_3$ catalyst is slightly smaller than that of Ni/bioSiC catalyst. The subtle distinction might be caused by the $Al_2O_3$ modification, which makes NiO better disperse on the support surface.

### 3.2. Performance of $Ni/Al_2O_3$, Ni/bioSiC and Ni/bioSiC–$Al_2O_3$ catalysts

The catalytic performance of $Ni/Al_2O_3$, Ni/bioSiC and Ni/bioSiC–$Al_2O_3$ catalysts was tested in a fixed-bed quartz reactor at 800 °C. The testing results are shown in Fig. 2. From the figure, $Ni/Al_2O_3$ catalyst shows an initial methane conversion of 92%, and the conversion rapidly decreases to 84% after 100 h. However, both Ni/bioSiC and Ni/bioSiC–$Al_2O_3$ catalysts exhibit higher catalytic activity and stability than $Ni/Al_2O_3$ catalyst. The initial methane conversion is 96% for Ni/bioSiC–$Al_2O_3$ and 92% for Ni/bioSiC catalyst. The higher catalytic activity of the $Al_2O_3$-modified catalyst possibly results from the higher surface area and the smaller size of metal particles. Most importantly, Ni/bioSiC–$Al_2O_3$ catalyst can steadily run more than 200 h without any drop of the methane conversion. In contrast, the activity of Ni/bioSiC catalyst exhibits a slow drop when the reaction time is longer than 50 h, and the methane conversion slowly decreases from the initial value to 88% at 200 h.

The CO and $H_2$ selectivity of Ni/bioSiC and Ni/bioSiC–$Al_2O_3$ catalysts is also shown in Fig. 3. From the figure, both of two catalysts exhibit high CO and $H_2$ selectivity. The CO selectivity of Ni/bioSiC–$Al_2O_3$ catalyst is about 99%, and it does not drop in the reaction. The $H_2$ selectivity is 96%, which is slightly low but does not show evident drop in the reaction. The initial CO selectivity of Ni/bioSiC catalyst is almost same with that of Ni/bioSiC–$Al_2O_3$ catalyst. However, the CO selectivity of Ni/bioSiC catalyst slowly drops with reaction time increasing. After 200 h, the CO selectivity decreases from the initial value to 97%. Similarly, the $H_2$ selectivity also shows a slow drop from 98% to 96%. Obviously, the alumina-modified catalyst has higher stability.

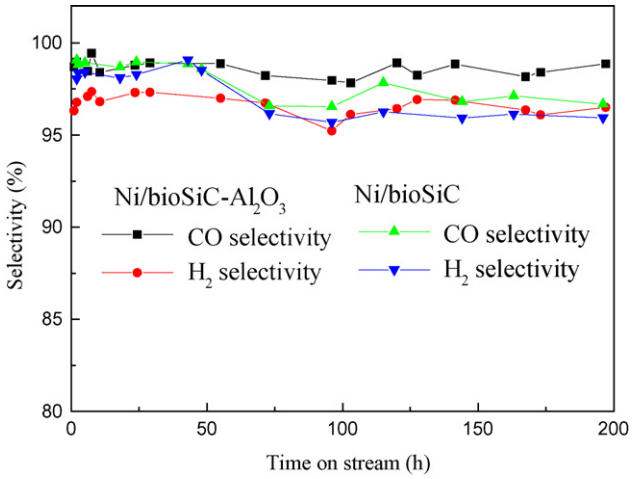


Fig. 3. CO and $H_2$ selectivity of Ni/bioSiC and Ni/bioSiC–$Al_2O_3$ catalysts at 800 °C.

### 3.3. TPR and ICP analysis

The TPR profiles of fresh Ni/bioSiC, Ni/bioSiC–$Al_2O_3$ and $Ni/Al_2O_3$ catalysts are shown in Fig. 4. From Fig. 4a, the reduction reaction of Ni/bioSiC catalyst starts from 280 °C and ends at 350 °C, which is lower than the reduction temperature (360 °C) of bulk NiO [31]. The low reduction temperature is mainly because that the NiO particles over SiC support have a very small size of about 23 nm, as demonstrated by the above XRD result. On the other hand, the low reduction temperature also indicates that the interaction between NiO and SiC is very weak. After the bioSiC support is modified by alumina, the TPR profile shows a similar initial reduction temperature to that of the unmodified catalyst and a much high ending temperature of about 800 °C, as shown in Fig. 4b. The low and wide reduction peak indicates that the alumina modification has enhanced the interaction between nickel and SiC support and the nickel component can exist in various active sites. From Fig. 4c, the reduction peaks of $Ni/Al_2O_3$ catalyst appear at about 400 °C and 700–900 °C. The higher reduction temperature indicates

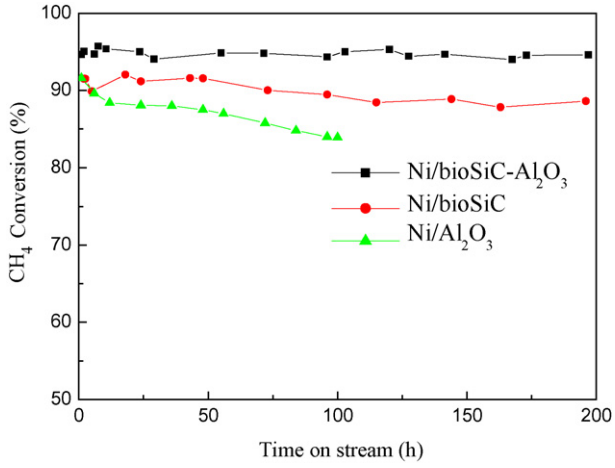


Fig. 2. Catalytic performance of $Ni/Al_2O_3$, Ni/bioSiC and Ni/bioSiC–$Al_2O_3$ catalysts at 800 °C.

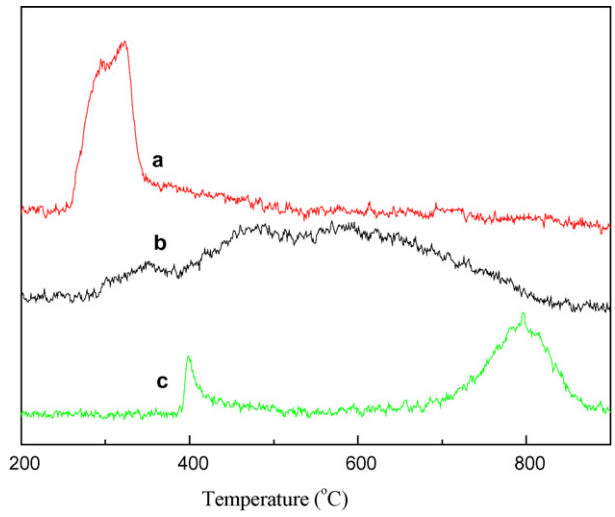


Fig. 4. TPR profiles of (a) Ni/bioSiC, (b) Ni/bioSiC–$Al_2O_3$ and (c) $Ni/Al_2O_3$ catalysts.

that the interaction between nickel and support for $Ni/Al_2O_3$ catalyst is higher than that for $Ni/bioSiC–Al_2O_3$ catalyst. The high temperature peak (~900 °C) is usually regarded as the reduction of $NiAl_2O_4$ produced in calcination [32]. Generally, the stronger interaction between nickel and support can effectively decrease the nickel loss. To confirm it, ICP analysis was used to measure the nickel loss of the two catalysts. After 200 h the nickel loss is 21% for Ni/bioSiC catalyst while 12% for $Ni/bioSiC–Al_2O_3$ catalyst. The results again demonstrate that the alumina modification makes nickel component more stable.

### 3.4. XRD and thermogravimetric analysis of used catalysts

To further investigate the effect of $Al_2O_3$ modification, the XRD technique was employed to characterize the used catalysts. From the XRD patterns shown in Fig. 5, the active phase of both catalysts has changed to metal Ni from NiO, which indicates that the reduced metal nickel is the active component for the POM reaction. The small peak at $2\theta = 26.7$ ($d = 3.335$ Å) results from deposited carbon, which encapsulates nickel particles and prevents them from oxidation. By thermogravimetric analysis, the carbon amount is 11.2 wt% for $Ni/bioSiC–Al_2O_3$ and 11.6 wt% for Ni/bioSiC catalysts. The two catalysts have almost same carbon deposition, and this indicates that the modification does not enhance the carbon deposition on the catalyst. Using Scherrer's formula, the crystalline size of metal nickel ((1 1 1) crystalline face) is 29.7 nm for $Ni/bioSiC–Al_2O_3$ and 47.2 nm for Ni/bioSiC. Obviously, the nickel particles over the unmodified SiC surface more easily migrate and grow.

The catalysts were prepared by impregnation method, through which nickel component was uniformly dispersed on the support surface. By calcination, the nickel component usually forms small particles that act as active sites in the POM reaction. For pure SiC support, these particles easily become large through migration and coalescence processes because the interaction between nickel and SiC support is too weak. As a result, the catalytic activity can decrease after a long time reaction. For $Ni/bioSiC–Al_2O_3$ catalyst, the interaction between active component and support has been enhanced by the alumina modification. The nickel particles on the modified surface are difficult to migrate and grow. Therefore, $Ni/bioSiC–Al_2O_3$ catalyst shows higher stability than Ni/bioSiC catalyst.

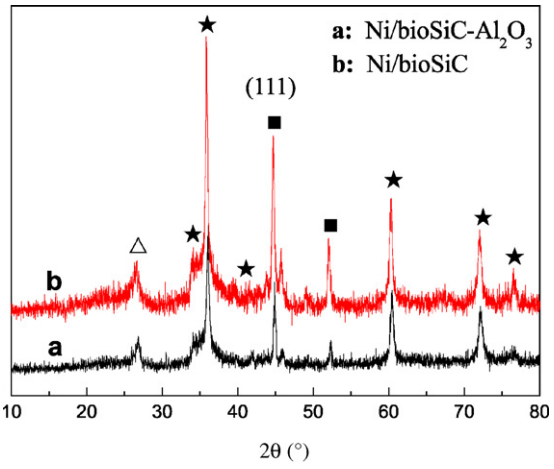


Fig. 5. XRD patterns of used catalysts. (★) SiC; (■) Ni; (△) carbon.

### 3.5. Performance of powdered and pelletized catalysts

The activities of powdered and pelletized $Ni/bioSiC–Al_2O_3$ catalysts were also investigated under different gas hourly space velocities (GHSV), as shown in Fig. 6. The powdered catalyst was prepared by loading NiO and $Al_2O_3$ on powdered SiC, which was obtained by milling the bioSiC pellets and had a specific surface area of 52.7 $m^2/g$. From the figure, the methane conversion is almost the same for the two catalysts when GHSV is 7500 $h^{-1}$. With increasing GHSV to 20,000 $h^{-1}$, the methane conversion decreases to 88% and 84%, respectively for the pelletized and powdered catalysts. Obviously, the pelletized catalyst at high GHSV exhibits higher activity than the powdered catalyst. bioSiC derived from carbonized millet possesses complex hierarchical alveolate structure, which is characterized by orderly arranged pores with various diameters ranging from nanometer to millimeter scale. It is a natural and perfect diffusion-reaction system, in which the microspores provide plentiful reaction surface while the large pores give effective diffusion channels. Therefore, $Ni/bioSiC–Al_2O_3$ catalyst can rapidly transport reactants to active sites and make them fully react at high GHSV. In contrast, there are not enough diffusion channels in the powdered catalyst, and the reactants are difficult to touch active sites and react on them. As a result, the catalytic activity of powdered catalyst is lower than that of the $Ni/bioSiC–Al_2O_3$ catalyst at high GHSV. Additionally, the pressure drop along the catalyst bed was also monitored. When GHSV increases from 7500 $h^{-1}$ to 20,000 $h^{-1}$, the pressure drop for the powdered catalyst increases from 0.2 atm to 0.6 atm. However, the reactor pressure for the pelletized catalyst almost does not change and the pressure drop remains a small value less than 0.1 atm.

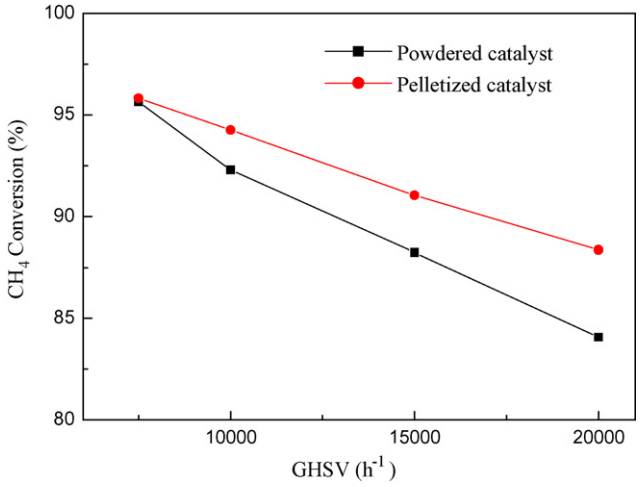


Fig. 6. Dependences of catalytic activity on gas hourly space velocity for powdered and pelletized catalysts.

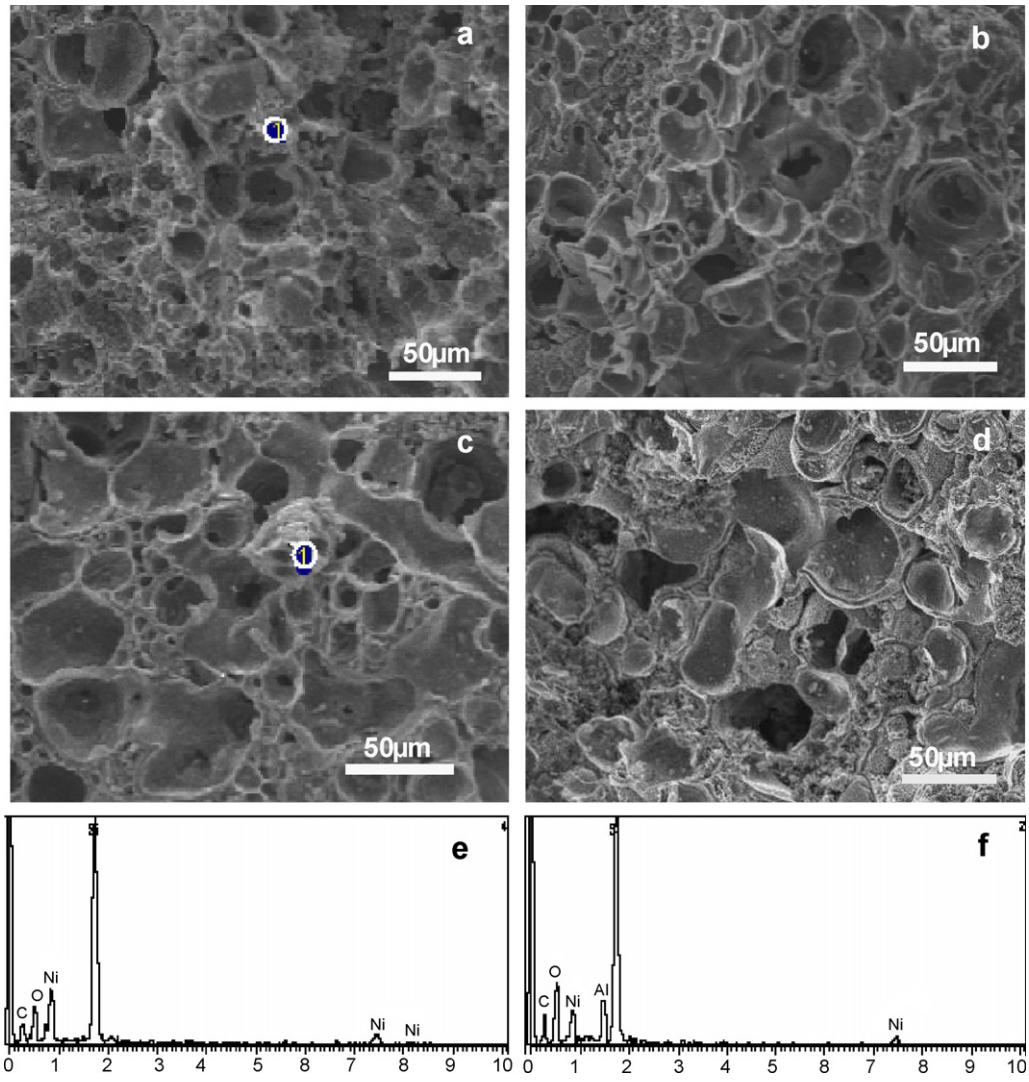


Fig. 7. SEM images and EDX spectra of catalysts before and after reaction. (a) Fresh and (b) used Ni/bioSiC catalyst; (c) fresh and (d) used Ni/bioSiC–$Al_2O_3$ catalyst; (e) and (f) EDX spectra of the circled areas in (a) and (c), respectively.

Therefore, one of the advantages of bioSiC as catalyst support is that it has a pellet dimension close to those of industrial catalysts and can be directly used in industrial processes without the shaping process.

### 3.6. SEM characterization

As discussed above, the superiority of bioSiC as the catalyst support mainly originates from the complex hierarchically porous structure. Therefore, it is important whether the porous structure can be remained or not in the POM reaction. Fig. 7a and c shows the SEM images of fresh Ni/bioSiC and Ni/bioSiC–$Al_2O_3$ catalysts, and both of them exhibit similar hierarchically porous structure. The EDX spectrum shown in Fig. 7e indicates that the elements in the randomly selected area (marked with circle) of the Ni/bioSiC catalyst interior are C, Si, Ni and O. Similarly, Fig. 7f shows that there exists Al element besides C, Si, Ni and O in Ni/bioSiC–$Al_2O_3$ catalyst. The EDX results demonstrate that nickel and alumina have infiltrated into the interiors of the two catalysts. Fig. 7b and d is SEM images of the two catalysts used after 200 h. The two images show that the porous structure of bioSiC pellets can be well remained in the POM reaction.

## 4. Conclusion

Alumina-modified biomorphic SiC pellets prepared from carbonized millet were employed as the catalyst support for partial oxidation of methane to syngas. The results showed that Ni/bioSiC–$Al_2O_3$ catalyst exhibited higher activity and stability than Ni/bioSiC catalyst. By XRD, TPR and ICP characterizations, it was demonstrated that the high activity and stability originated from the alumina modification. The modification greatly enhanced the interaction between nickel and support and therefore prevented the growth and loss of nickel particles on the support. The performance of powdered and pelletized Ni/bioSiC–$Al_2O_3$ catalysts was also investigated at different gas hourly space velocities. It was found that the pelletized catalyst had higher catalytic activity at high gas hourly space velocity. The SEM results showed that the

hierarchically porous structure of bioSiC pellets could be well remained after 200 h. From the above results, it is concluded that due to the high mechanical strength and chemical stability the biomorphic SiC with hierarchically porous structures will be an excellent catalyst support, especially for applications in harsh environments.

## Acknowledgement

The work is financially supported by National Nature Science Foundation of China (Grant No. 20471067).

## References

[1] T. Takeguchi, S.N. Furukawa, M. Inoue, J. Catal. 202 (2001) 14.
[2] K. Heitnes, S. Lindberg, O.A. Rokstad, A. Holmen, Catal. Today 24 (1995) 211.
[3] Q.G. Yan, W.Z. Weng, H.L. Wan, H. Toghiani, R.K. Toghiani, C.U. Pittman, Appl. Catal. A 239 (2003) 43.
[4] Y.H. Zhang, G.X. Xiong, S.S. Shan, W.S. Yang, Catal. Today 63 (2000) 517.
[5] J.H. Jun, T.J. Lee, T.H. Lim, S.W. Nam, S.A. Hong, K.J. Yong, J. Catal. 221 (2004) 178.
[6] A. Basile, L. Paturzo, F. Lagana, Catal. Today 67 (2001) 65.
[7] S. Albertazzi, P. Arpentinier, F. Basile, P. Del Gallo, G. Fornasari, D. Gary, A. Vaccari, Appl. Catal. A 247 (2003) 1.
[8] S. Takenaka, H. Umebayashi, E. Tanabe, H. Matsune, M. Kishida, J. Catal. 245 (2007) 390.
[9] W.S. Dong, K.W. Jun, H.S. Roh, Z.W. Liu, S.E. Park, Catal. Lett. 78 (2002) 215.
[10] M. Soick, O. Buyevskaya, M. Hohenberger, D. Wolf, Catal. Today 32 (1996) 163.
[11] J. Requies, M.A. Cabrero, V.L. Barrio, M.B. Guemez, J.F. Cambra, P.L. Arias, F.J. Perez-Alonso, M. Ojeda, M.A. Pena, J.L.G. Fierro, Appl. Catal. A 289 (2005) 214.
[12] U. Olsbye, O. Moen, A. Slagtern, I.M. Dahl, Appl. Catal. A 228 (2002) 289.
[13] D. Dissananayake, M.P. Rosenek, K.C.C. Kharas, J.H. Lunford, J. Catal. 132 (1991) 117.
[14] Z.W. Liu, K.W. Jun, H.S. Roh, S.C. Baek, S.E. Park, J. Mol. Catal. A 189 (2002) 283.
[15] Y.J. Hao, G.Q. Jin, X.D. Han, X.Y. Guo, Mater. Lett. 60 (2006) 1334.
[16] N. Keller, C. Pham-Huu, C. Estournes, M.J. Ledoux, Appl. Catal. A 234 (2002) 191.
[17] M.E. Harlin, A.O.I. Krause, B. Heinrich, C. Pham-Huu, M.J. Ledoux, Appl. Catal. A 185 (1999) 311.
[18] R. Moene, M. Makkee, J.A. Moulijn, Appl. Catal. A 167 (1998) 321.
[19] J.M. Nhut, L. Pesant, N. Keller, C. Pham-Huu, M.J. Ledoux, Top. Catal. 30/31 (2004) 353.
[20] P. Leroi, B. Madani, C. Pham-Huu, M.J. Ledoux, S. Savin-Poncet, J.L. Bousquet, Catal. Today 91/92 (2004) 53.
[21] W.Z. Sun, G.Q. Jin, X.Y. Guo, Catal. Commun. 6 (2005) 135.
[22] H. Sieber, C. Hoffmann, A. Kaindl, P. Greil, Adv. Eng. Mater. 2 (2000) 105.
[23] C.R. Rambo, J. Cao, O. Rusina, H. Sieber, Carbon 43 (2005) 1174.
[24] Q. Wang, G.Q. Jin, D.H. Wang, X.Y. Guo, Mater. Sci. Eng. A 459 (2007) 1.
[25] P. Greil, J. Eur. Ceram. Soc. 21 (2001) 105.
[26] J.M. Qian, J.P. Wang, G.J. Qiao, Z.H. Jin, J. Eur. Ceram. Soc. 24 (2004) 3251.
[27] M. Sheintuch, Chem. Eng. Sci. 55 (2000) 615.
[28] C. Gavrilov, M. Sheintuch, AIChE J. 43 (1997) 1691.
[29] J. Cao, C.R. Rambo, H. Sieber, Ceram. Int. 30 (2004) 1967.
[30] W.Z. Sun, R.F. Mo, G.Q. Jin, X.Y. Guo, Nat. Gas Chem. Ind. 31 (2006) 1.
[31] J.A. Montoya, E. Romero-Pascual, C. Gimon, P. Del Angel, A. Monzon, Catal. Today 63 (2000) 71.
[32] T.H. Wu, A.B. Li, Q.G. Yan, Chinese J. Catal. 22 (2001) 501.